Analysis of the Inhibition Layer of Galvanized Dual-Phase Steels

K.-K. Wang, H.-P. Wang, L. Chang, D. Gan, T.-R. Chen[1,†], and H.-B. Chen[1]

Department of Materials and Optoelectronic Science,
National Sun Yat-Sen University, Kaohsiung 80424, Taiwan, R. O. C.
[1]Steel & Aluminum R&D Department,
China Steel Corporation, Kaohsiung 81233, Taiwan, R. O. C.

The formation of the Fe-Al inhibition layer in hot-dip galvanizing is a confusing issue for a long time. This study presents a characterization result on the inhibition layer formed on C-Mn-Cr and C-Mn-Si dual-phase steels after a short time galvanizing. The samples were annealed at 800 ℃ for 60 s in N_2-10% H_2 atmosphere with a dew point of -30 ℃, and were then galvanized in a bath containing 0.2 %Al. X-ray photoelectron spectroscopy (XPS) and transmission electron microscopy (TEM) was employed for characterization. The TEM electron diffraction shows that only Fe_2Al_5 intermetallic phase was formed. No orientation relationship between the Fe_2Al_5 phase and the steel substrate could be identified. Two peaks of Al 2p photoelectrons, one from metallic aluminum and the other from Al^{3+} ions, were detected in the inhibition layer, indicating that the layer is in fact a mixture of Fe_2Al_5 and Al_2O_3. TEM/EDS analysis verifies the existence of Al_2O_3 in the boundaries of Fe_2Al_5 grains. The nucleation of Fe_2Al_5 and the reduction of the surface oxide probably proceeded concurrently on galvanizing, and the residual oxides prohibited the heteroepitaxial growth of Fe_2Al_5.

Keywords : inhibition layer, galvanizing, dual-phase steel, oxides

1. Introduction

Hot dip galvanized/galvannealed dual-phase (DP) steel has become one of the most important materials in car manufacturing to fulfill the requirements of fuel economy, crashworthiness and corrosion resistance. However, it is well known that most of the alloy elements, such as Mn, Si, and Cr, added in dual-phase steels for increased hardenability exhibit high oxide formation tendencies so that selective oxidation occurs upon intercritical annealing even though protective atmosphere is employed.[1)-3)] The oxides are believed to deteriorate the wettability of liquid Zn and hinder the formation of Fe-Al inhibition layer during continuous hot-dip galvanizing process.[4)-7)] A uniformly distributed inhibition layer prohibits the nucleation and growth of brittle Fe-Zn intermetallics and ensures good adherence of the galvanized coating. In addition, the formability and surface appearance of the galvannealed coating is closely related to the quality of the inhibition layer which controls the homogeneity of the Fe-Zn interfacial reactions. However, the formation mechanism of the Fe-Al (-Zn) in-

hibition layer on low carbon (LC) steels and interstitial free (IF) steels is still elusive, though both of which have been used for outer-panels for years.[8)-12)] As a result, the understanding of the microstructures and the formation mechanism of the inhibition layer on the DP steels is very limited. Tobiyama and Kato[13)] reported that the thickness of the inhibition layer decreased with increasing Mn or Si contents in the steels. The co-existence of Mn and Si allows the formation of Mn_2SiO_4 oxides on the steel surface during annealing which is detrimental to the formation of inhibition layer.[6)] On the other hand, Khondker et al.[14)] suggested that manganese oxides can be reduced by Al in the bath and may not hinder the Fe-Al reaction(s). A mechanism involving the aluminothermic reduction of MnO followed by a two-step formation of the inhibition layer on high Al-low Si TRIP (transformation-induced plasticity) steels was proposed recently.[15)]

We reported recently results by in-plane transmission electron microscopy (TEM) analysis of the inhibition layer formation on a TiNb-added IF steel.[16)] By dissolving chemically the Fe and Zn away, large area of the inhibition layer and residual substrate is available for microscopic observation. A well-defined orientation relationship be-

† Corresponding author: t11c1@mail.csc.com.tw

tween the steel substrate and the Fe_2Al_5 compound was observed, indicating Fe_2Al_5 forms via a heterogeneous epitaxial growth on a iron. In this study, the same methodology was employed to characterize the inhibition layer formed on dual phase steels. Additional x-ray photoelectron spectroscopy (XPS) analysis was carried out to collect chemical information.

2. Experimental details

Two steels, a C-Mn-Cr steel and a C-Mn-Si steel, with compositions listed in Table 1 were prepared by vacuum induction melting. The ingots went through a series of processes to simulate the hot rolling, coiling, cold rolling and continuous annealing/hot-dip galvanizing in sequence. The ingots were first reheated and soaked at 1250 ℃ for two hours, and were hot rolled in nine sequential passes without interruption to a thickness of approximately 5 mm. The finish-rolling temperature was 880 ℃. The strips were rapidly cooled by water spray to about 500 ℃ and then immediately soaked at 550 ℃ in a furnace followed by a controlled cooling process to the room temperature to simulate the coiling process. After the coiling simulation, the hot bands were machined to a thickness of 4 mm to remove the scale and then cold rolled to 1.0 mm thick (cold reduction=75%). After being electrolytically cleaned, cold-rolled samples of 120 mm x 200 mm in size were loaded separately in a commercial hot-dip simulator (Iwatani EU4) and were annealed at 800 ℃ for 60 seconds in a $N_2 + 10$ % H_2 atmosphere with a dew point of -30 ℃. Some samples were cooled and taken out at this stage for XPS analysis of surface oxides. Other samples were then galvanized by cooling to 460 ℃ at a rate of 15 ℃/s, holding for 10 s and then dipping into a Zn bath containing 0.2 wt% Al for 4 s. Nitrogen gas jet was used to blow out excess Zn when samples were withdrawn from the Zn bath to form a Zn coating of average weight 45 g/m². The Zn bath, slightly undersaturated with iron (0.011 wt%), contained 0.19 wt% of aluminum as analyzed by spark optical emission spectroscopy. The temperature of the Zn bath was controlled to 460 +/-2 ℃.

The specimens used for characterization of inhibition layer were cut from the uniform coating area at the center of the galvanized sample. Samples were then dipped into

Table 1. Chemical composition [in wt%] of the steels used in this study

Steel	Mn	Cr	Si	Al	C	P	N
C-Mn-Cr	1.02	1.02	0.02	0.043	0.10	0.017	0.0051
C-Mn-Si	2.01	-	0.5	0.043	0.10	0.017	0.0051

diluted hydrochloric acid to remove the Zn coating to expose the Fe-Al compound. Samples for XPS (JEOL JPS9010MX) analysis were sputtered by 2 kV Ar ions for 50 seconds to remove oxides formed on etching. Non-monochromatized Mg K$_a$ x-ray beam is used to radiate the sample, and the core level spectrum for each element was collected in 0.2 eV step and at a 10 eV pass energy. For TEM (FEI Tecnai G2 operating at 200 kV) observation, Zn was first removed as above, followed by evaporating a thin layer of amorphous carbon onto the thin intermetallic compound to strengthen it, and then the Fe substrate was removed by chemical dissolution and the compound layer was placed on Cu grid. To study the orientation relationship between Fe substrate and Fe-Al compound, the Fe removal process was stopped before completion so that a thin layer of Fe was retained.

3. Results and discussion

Fig. 1 shows the XPS core level spectra for Mn $2p_{3/2}$, Cr $2p_{3/2}$, Si 2p and Al 2p acquired from the as-annealed samples and the galvanized samples. Spectra acquired from sintered Mn_3O_4, Al_2O_3 and Cr_2O_3 standards are also included for references. The Mn $2p_{3/2}$ spectrum for the C-Mn-Cr steel in the as-annealed state (Fig. 1a) is very similar to that for the Mn_3O_4 standard, containing two component peaks at 640.5 eV and 642.2 eV. Considering the fact that the binding energy of Cr $2p_{3/2}$ peak for the annealed C-Mn-Cr sample in Fig. 1b deviated slightly from that for Cr_2O_3, the oxides formed on the steel surface are possibly a mixture of manganese oxides, Mn_3O_4 and $MnCr_2O_4$ spinel. This is proved by TEM results described later. For the annealed C-Mn-Si steel, Mn $2p_{3/2}$ spectrum has a strong component at 642.2 eV (Fig. 1a) and the Si 2p peak is at 101.8 eV (Fig. 1c), both the characteristics agreeing well with those for Mn-Si mixed oxides, such as Mn_2SiO_4.[1),2)] The oxides formed on the C-Mn-Si steel are therefore a mixture of manganese oxides, probably Mn_3O_4 and Mn_2SiO_4.

The Zn coating on the galvanized samples was removed for XPS analysis. All the Fe $2p_{3/2}$ peaks (results not shown) are in the metallic state, confirming that the oxides formed during on etching have been removed by sputtering. In Fig. 1a, a weak Mn peak is recognized for the galvanized C-Mn-Cr sample and a relatively strong Mn peak at 642 eV is resolved for the galvanized C-Mn-Si sample. In Fig. 1b, Cr $2p_{3/2}$ peak at 576.4 eV is detected in the inhibition layer of the galvanized C-Mn-Cr steel, showing that the inhibition layer contains $MnCr_2O_4$. Fig. 1c shows that no Si peak can be recognized for the galvanized C-Mn-Si sample. However, considering the Mn peak at 642 eV
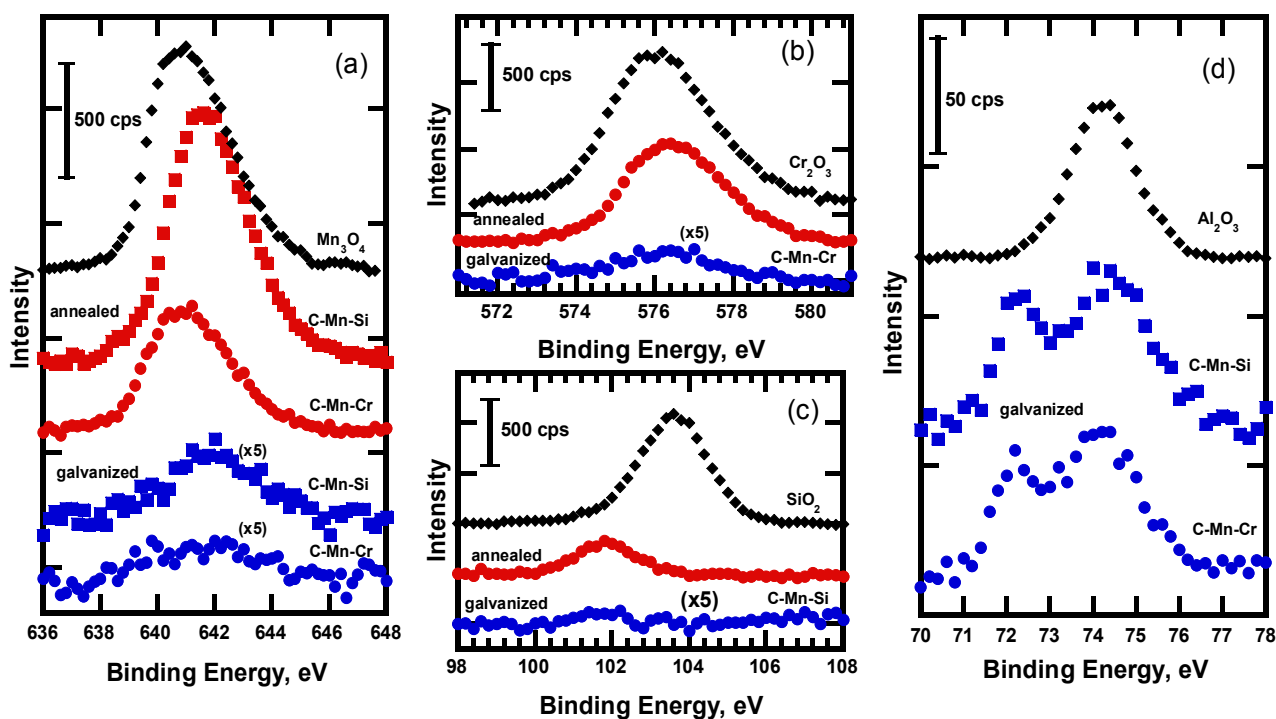
Figure 1. XPS spectra for (a) Mn 2p$_{3/2}$, (b) Cr 2p$_{3/2}$, (c) Si 2p, and (d) Al 2p acquired from the as-annealed and the galvanized C-Mn-Cr and C-Mn-Si samples.

shown in Fig. 1a, the inhibition layer of the C-Mn-Si sample may contains small amount of Mn_2SiO_4. Accordingly, the external oxides containing Cr or Si are at least partially retained in the inhibition layer of both samples. Fig. 1d shows that two Al 2p peaks, one for metallic Al at 72.5 eV and another for Al^{3+} of Al_2O_3, are observed for both samples. The inhibition layer is indeed composed of a mixture of Fe-Al intermetallic phase(s), Al_2O_3 and Cr or Si containing oxides.

Figs. 2a-d are the TEM bright field image, diffraction pattern, energy dispersive X-ray spectrum and dark field image of inhibition layers extracted from the galvanized C-Mn-Cr sample. The ring pattern in Fig. 2b is identified to be the orthorhombic Fe_2Al_5 phase and the indexes are shown. Energy dispersive X-ray spectroscopy (EDS) analysis (Fig. 2c) showed that the layer contains about 5 at% Zn and, consequently, the inhibition layer is a ternary $Fe_2Al_{5-x}Zn_x$ compound. It is worth noting that C, O, Cr, Si, Mn and Cu are also detected in the inhibition layer. The C signal is contributed from the carbon coating applied for extracting the inhibition layer, and the Cu signal is resulted from the stray radiation. However, the rest elements are not expected to exist in the inhibition layer and the phenomenon will be discussed later. The dark field image of Fig. 2d was formed with a portion of the diffraction rings and shows that the grain size of $Fe_2Al_{5-x}Zn_x$

changes widely from ~50 nm to as large as 500 nm. It is also worth mentioning that the thickness of the inhibition layer is not uniform. $Fe_2Al_{5-x}Zn_x$ grains of large sizes tend to aggregate in thick portion. In addition, no orientation relationship was observed between $Fe_2Al_{5-x}Zn_x$ and steel substrate in contrast to a well-defined orientation relationship between Fe_2Al_5 and IF steel, as reported by us previously.[16] Similar phenomena were also observed for the C-Mn-Si steels.

Fig. 3a shows a bright field image obtained at a high magnification for the inhibition layer formed on the galvanized C-Mn-Si steel. It is evident that the layer is composed of coarse grained $Fe_2Al_{5-x}Zn_x$ (>200 nm) in thick region and fine grained $Fe_2Al_{5-x}Zn_x$ (<100 nm) in thin region. Two EDS spectra acquired from positions 1 (thick region) and position 2 (thin region) are shown in Fig. 3b. The spectrum acquired from position 1 is free from oxygen. In contrast, the oxygen content in the thin region (position 2) is high and a Si peak is also detected. Accordingly, it can be inferred that the Al_2O_3 and Mn_2SiO_4 are distributed mainly in the thin portion of the inhibition layer.

The nucleation and growth of $Fe_2Al_{5-x}Zn_x$ is therefore closely related to the oxides formed on the steel surface prior to galvanizing. The oxides are shown in Fig. 4a of the annealed C-Mn-Cr steel which reveals that the steel
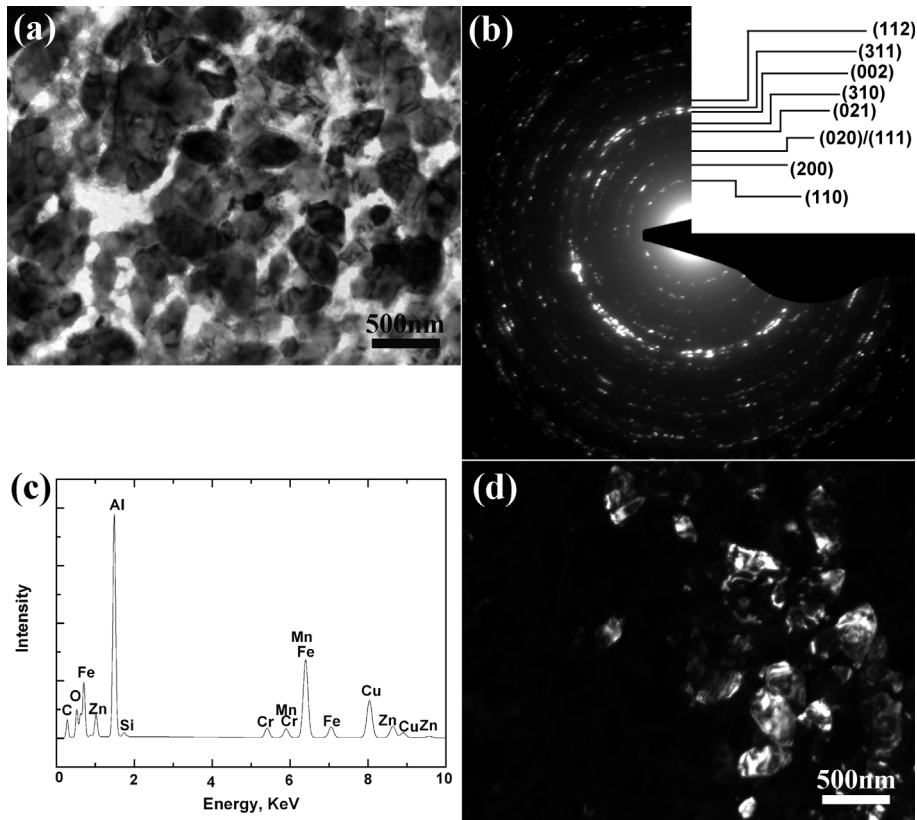
Figure 2. Microstructures and diffraction patterns of the inhibition layer formed on the galvanized C-Mn-Cr steels. (a) TEM bright field image, (b) selected area ring pattern and corresponding indexes, (c) energy dispersive X-ray spectrum and (d) dark field image formed with a portion of the SAD ring in (b).
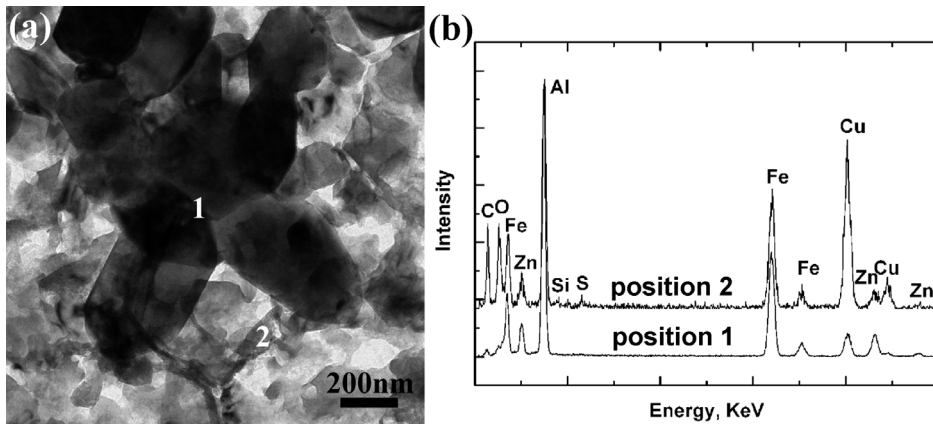
Figure 3. (a) Bright field image of the inhibition layer formed on the galvanized C-Mn-Si steel. (b) Corresponding energy dispersive spectra acquired from position 1 and position 2 in (a).

surface is only partially covered. The oxides consist mainly of Mn_3O_4 and $MnCr_2O_4$ according to the corresponding diffraction pattern in Fig. 4b. Several reactions might occur concurrently in galvanizing. First, the iron in contact with the liquid zinc dissolved and was followed by the nuclea-

tion of the $Fe_2Al_{5-x}Zn_x$ phase at the interface. Second, manganese oxides on the surface were quickly reduced by Al in the Zn bath according to the so-called aluminothermic reduction reaction:[14]
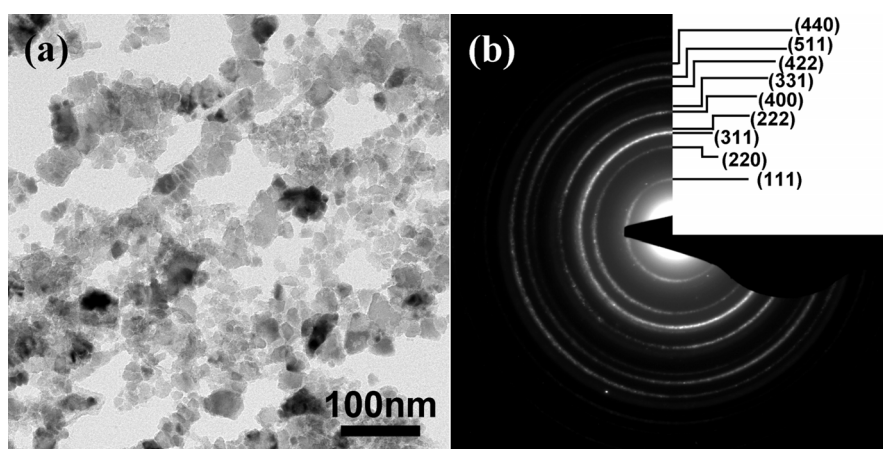
Figure 4. (a) Bright field image and (b) corresponding diffraction patterns of oxides extracted from the annealed C-Mn-Cr sample.

$$3Mn_xO_{y(s)} + 2yAl_{(in\ Zn)} \rightarrow yAl_2O_{3(s)} + 3xMn_{(in\ Zn)}$$
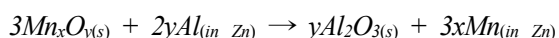
The reduced Mn then dissolved into the Zn bath and diffused outwards rapidly. The resultant Al_2O_3 particles, on the other hand, were trapped in the inhibition layer during the growth and coalescence of $Fe_2Al_{5-x}Zn_x$ grains. Third, a portion of oxides, such as $MnCr_2O_4$ and Mn_2SiO_4, which could not be or had not been reduced by Al, were detached from the interface due to the dissolution of underneath iron and are trapped in the inhibition layer, too. The detachment of $MnCr_2O_4$ and Mn_2SiO_4 allows new $Fe_2Al_{5-x}Zn_x$ grains to nucleate on the newly exposed steel surface.

When the steel was dipped into the bath, the $Fe_2Al_{5-x}Zn_x$ grains nucleated rapidly on the uncovered steel surface. These $Fe_2Al_{5-x}Zn_x$ grains had longer time to grow and therefore had large sizes (Fig. 3a). For the portion of substrate covered by oxides, Al was depleted and the formation of $Fe_2Al_{5-x}Zn_x$ was rather sluggish. The inhibition layer was therefore thin and was composed of fine grained $Fe_2Al_{5-x}Zn_x$. The Al_2O_3 and remaining unreduced oxides, such as $MnCr_2O_4$ and Mn_2SiO_4, were incorporated and resulted in the oxygen and silicon peaks in EDS of Fig. 3b.

Unlike the case for the galvanized IF steel,[16] no orientation relationship between the $Fe_2Al_{5-x}Zn_x$ intermetallic and the steel substrate was observed. This could be attributed to the fact that dual phase steels usually possess a weak recrystallization texture and the population of steel grains having preferential orientations of <110> and <111> parallel to the normal direction is low.[18),19)] Moreover, the various oxides observed on the DP steels could surely disrupt the epitaxial nucleation of $Fe_2Al_{5-x}Zn_x$ with respect to the steel surface. Therefore, these $Fe_2Al_{5-x}Zn_x$ grains did not have any crystallographic orientation relation with the steel substrate.

4. Summary

In summary, the formation of the inhibition layer of galvanizing dual phase steels in Al-containing Zn bath was studied. Prior to the galvanizing, the steel surface was partially covered by manganese oxides and Cr or Si containing oxides. XPS and TEM results all showed that significant amount of oxides existed in the inhibition layer. The oxides included $MnCr_2O_4$ or Mn_2SiO_4 formed during annealing and Al_2O_3 formed in the reduction of manganese oxides by Al in the zinc bath. The depletion rate of Al on reducing manganese oxides played a key role on retarding the nucleation and growth of $Fe_2Al_{5-x}Zn_x$ at the oxides covered surface. The inhibition layer was composed of mixed thick and thin regions. The thick regions contained coarse $Fe_2Al_{5-x}Zn_x$ grains formed in the beginning of galvanizing and the thin regions were a mixture of oxides and fine grained $Fe_2Al_{5-x}Zn_x$ formed in the late stage. No orientation relationship was observed between the $Fe_2Al_{5-x}Zn_x$ and the steel substrate.

Acknowledgments

References

1. X. Vanden Eynde, J. P. Servais, and M. Lamberigys,

Surf. Interf. Anal., **35**, 1004 (2003).

2. S. Swaminathan and M. Spiegel, *Appl. Surf. Sci*., **253**, 4607 (2007).

3. H. J. Grabke, V. Leroy, and H. Viefhaus, *ISIJ Int*., **35**, 95 (1995).

4. M. Isobe, C. Kato, and K. Mochizuki, *Proc. 39th Mechanical Working and Steel Processing* (*MWSP*) *Conf*., p. 121, Iron and Steel Society (1998).

5. B. Mintz, *Inter. Mater. Rev*., **46**, 169 (2001).

6. J. Mahieu, S. Claessens, and B. C. De Cooman, *Metall. Mater. Trans. A*, **32A**, 2905 (2001).

7. Y. Tobiyama, Y. Suzuki, K. Kyono, and C. Kato, *Galvatech '04*, p. 771, AIST, Warrendale, PA (2004).

8. M. Guttmann, Y. Lepretre, A. Aubry, M.-J. Roche, T. Moreau, P. Drillet, J. M. Mataigne, and H. Baudin, *Galvatech '95*, p. 295, Iron and Steel Society (1995).

9. G. J. Harvey and P. D. Mercer, *Metall. Trans*., **4**, 619 (1973).

10. N.-Y. Tang and G. R. Adams, in: A.R. Marder (Ed.), The Physical Metallurgy of Znic Coated Steel, p. 41, TMS, Warrendale, PA (1994).

11. E. McDevitt, Y. Morimoto, and M. Meshii, *ISIJ Int*., **37**, 776 (1997).

12. L. Chen, R. Fourmentin, and J. McDermid, *Galvatech '07*, p. 321, Iron and Steel Institute of Japan (2007).

13. Y. Tobiyama and C. Kato, *Tetsu-to-Hagane*, **89**, 38 (2003).

14. R. Khondker, A. Mertens, and J. R. McDermid, *Mater. Sci. Eng. A*, **463**, 157 (2007).

15. E. M. Bellhouse and J. R. McDermid, *Mater. Sci. Eng. A*, **491**, 39 (2008).

16. K.-K. Wang, L. Chang, D. Gan, and H.-P. Wang, *Thin Solid Films* (in press).

17. H.-P. Wang, K.-K. Wang, L. Chang, D. Gan, T.-R. Chen, H.-B. Chen, and K.-C. Yang, *Proc. Taiwan 2008 ISTS Conf*., China Steel Corp., Kaohsiung, Taiwan, A27 (2008).

18. R. K. Ray, *Mater. Sci. Eng. A*, **77**, 169 (1986).

19. S. G. Chowdhury, E. V. Pereloma, and D. B. Santos, *Mater. Sci. Eng. A*, **480**, 540 (2008).